



Elastic organic crystals of π -conjugated molecules: anisotropic densely packed supramolecular 3D polymers exhibit mechanical flexibility and shape tunability

Shotaro Hayashi ¹

Received: 10 March 2019 / Revised: 31 March 2019 / Accepted: 2 April 2019 / Published online: 25 April 2019
© The Society of Polymer Science, Japan 2019

Abstract

π -Conjugated molecules have attracted much attention over recent years and have applications in various organic devices. Single crystals of these molecules are attractive materials for developing unique and/or high-performance devices owing to their anisotropic densely packed supramolecular 3D polymer structures. However, they are not flexible and are therefore not suitable for wearable devices. In this focus review, the author's recent work on flexible crystals involving designing fibril lamella of slip-stacked molecular wires based on planar π -conjugated molecules and their applications is summarized. Unlike common organic crystals, 1,4-bis[2-(4-methylthienyl)]-2,3,5,6-tetrafluorobenzene exhibits elastic bending flexibility with π -functionality. This supramolecular 3D polymer design concept offers top-down synthesis of crystalline fibers and films. Moreover, the functionality and flexibility of such a crystal realizes both high-performance flexible fluorescent waveguide and reversible mechanofluorochromic behavior. Finally, the interesting shape-tunable supramolecular formation of a fluorescent π -conjugated polymer containing a 1,4-bis[2-(4-hexylthienyl)]-2,3,5,6-tetrafluorobenzene repeating unit is described.

Introduction

The importance of π -conjugated molecules (π CMs) has increased over the last few decades [1–3], resulting in the design and synthesis of a variety of π CMs [4–10]. The formation of supramolecular assemblies of π CMs has attracted considerable attention in the soft materials research field [11–13]. In this field, the formation of architectures with long-range ordering depends on the effective recognition or interaction between rationally designed molecules. π -Stacking and other monomer interactions give various supramolecular polymers (Fig. 1a). One-dimensional growth mainly involving the π -stacking of π CMs gives nanofibers as supramolecular 1D polymers (Fig. 1b) [14, 15]. The difficulty of the controlling the alignment of the nanofibers is similar to common polymers made with covalent bonds, thus resulting in a lack of anisotropy and

density on a macroscopic scale. The two-dimensional growth of the organic molecules gives crystalline films as supramolecular 2D polymers (Fig. 1c) [16, 17]. Thin films consisting of one or a few molecular layers often show flexibility similar to common polymer films. The three-dimensional growth of π CMs gives bulk single crystals (Fig. 1d). Because these are highly ordered 3D molecular assemblies brought together by noncovalent bonding, they will be called here supramolecular 3D polymers. These materials have attracted much attention owing to their anisotropic densely packed molecular structures, which offer a high refractive index and charge transportation properties [18–20]. However, it is well known that these crystals are not flexible and are mechanically weak [21, 22].

Organic single crystals of π CMs are anisotropic and densely packed molecular assemblies and have an important role in optoelectronic devices and sensors [23–25]. The defect-free alignment with dense packing of π CMs contributes to their excellent performance in devices. However, organic crystals are often brittle, making it difficult to create flexible devices with crystalline organic materials. However, π -conjugated polymers [26–30] offer flexible fibers and films, but these materials sometimes contain amorphous domains and defects [31–33]. Consequently, flexible and

✉ Shotaro Hayashi
shayashi@nda.ac.jp

¹ Department of Applied Chemistry, National Defense Academy, 1-10-20 Hashirimizu, Yokosuka, Kanagawa 239-8686, Japan

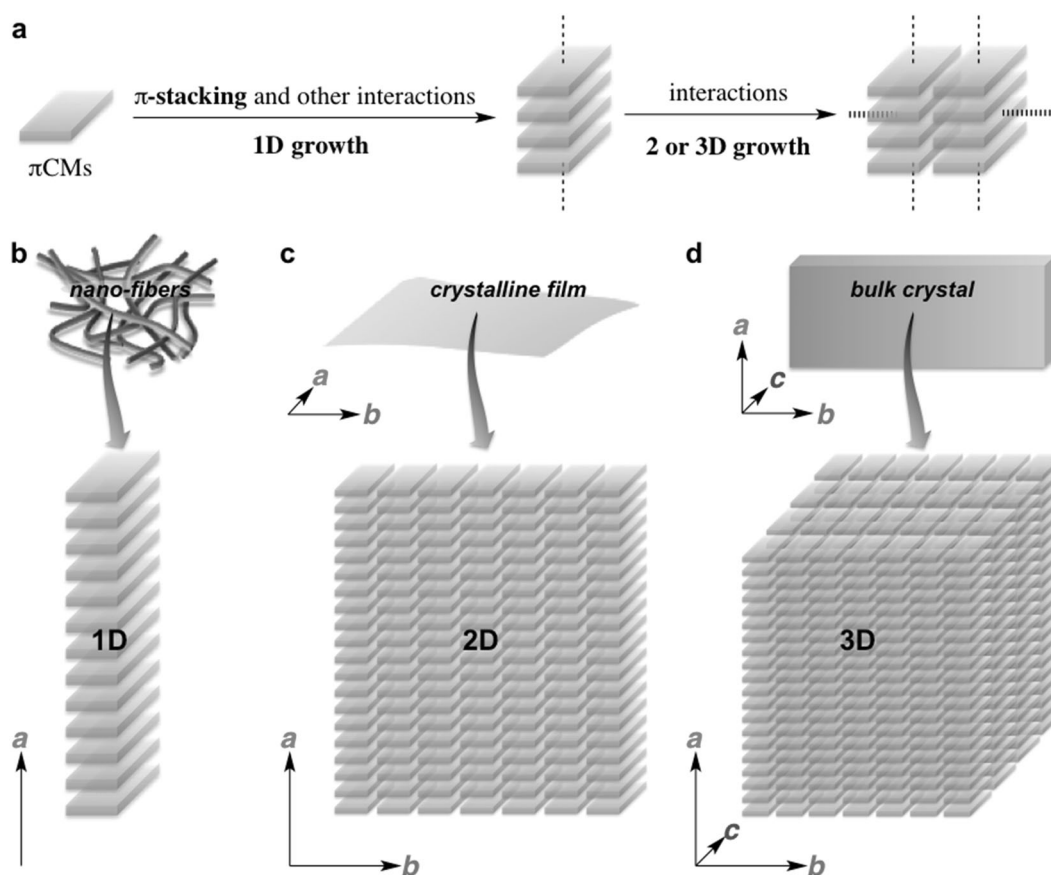


Fig. 1 **a** Self-assembly of π -conjugated molecules into supramolecular polymers. **b** Nanofibers. **c** Crystalline thin film. **d** Bulk single crystals

tough crystals of π CMs are candidate materials for high-performance flexible devices and mechanosensors. Thus, research into flexible organic crystals under bending stress has received considerable attention in recent years [34]. Bendable organic crystals occasionally show irreversible (plastic) deformation under applied stress [35]. On the other hand, reversible (elastic) bending of organic single crystals is a rare phenomenon, and it has only been shown in a few recent reports [36]. The development of novel π -conjugated molecular frameworks with improved and reliable performance is necessary for practical applications.

Elastic organic crystals of π -CMs

Fibril lamella based on stretchable wires are known to give dense and flexible materials that are found in nature, including the muscle tissue of animals and the scales of fish [37]. The author hypothesizes that π -CMs suitable for elastic organic crystals require: (i) a planar conformation, (ii) a rigid structure, and (iii) controlled intermolecular interactions for face-to-face slip-stacking. The molecular sliding in slip-stacking is a candidate for stretchable

molecular wires in fibril lamella. This target structure is exemplified by fibers based on a fibril lamella morphology of slip-stacked molecular wires (Fig. 2).

For the preparation of elastic crystals meeting the aforementioned criteria (i–iii), research focused on oligothiophene molecules with a tetrafluorobenzene core. The sulfur atom in the thiophene and the fluorine atom on the tetrafluorobenzene provide the four intramolecular hydrogen bonds, [H...F_a], and contacts, [S...F_b], that would yield a highly planar and rigid molecular structure [38–40]. Moreover, crystal structures based on the slip-stacking of related oligothiophene molecules have also been reported. The author designed 1,4-bis[2-(4-methylthienyl)]-2,3,5,6-tetrafluorobenzene, **1**, which was synthesized by a palladium-catalyzed Stille cross-coupling reaction and gives centimeter-scale single crystals (Fig. 3) [41–43]. The crystal structure of **1** contains S...F and F...H intramolecular interactions that are significantly shorter than the sums of their van der Waals radii (Fig. 3a, b). These contacts result in highly planar molecules with a maximum torsion angle of 1.27° between the tetrafluorophenylene and thiophene units. The molecules form a slip-stacked assembly with a center-to-center separation between the thiophene–tetrafluorobenzene–thiophene planes of 2.347 Å

(Fig. 3c). The fibril lamella morphology originates from the slip-stacked molecular wires at the (010) and (001) faces through self-assembly of the planar tetrafluorophenylene–thiophene molecules (Fig. 3c). To clearly observe the macroscopic elastic bending, the author investigated the mechanical performance of the crystal under UV irradiation at 365 nm (Fig. 3d). The straight crystal (i) bent under applied stress (ii–vi) and relaxed upon stress reduction

(vii and viii) to recover its original shape. The crystal bending angle exceeded 180° (vi). This reversible bending–relaxation of the crystal could be cycled many times.

Mechanically induced shaping of micro- and nanofibers

Supramolecular 3D polymer materials, especially crystals, of π -CMs have attracted considerable research attention owing to their potential applications in organic devices [44–46]. The macroscopic shapes of the crystals of π -CMs are important for the development of device applications, and depend on bottom–up processes. Consequently, it is difficult to intentionally control their shapes. Top–down processing (i.e., forming small crystals from larger ones) is a very practical method for crystal shape control, but it is only feasible for soft and flexible materials. Typical soft materials, such as polymers, are of great interest as their flexibility allows them to form various shapes via facile mechanical shaping. However, unlike polymer materials, applying stress to common organic single crystals generally causes them to disintegrate into powders and crystallites.

Thermal- or photochemical stimuli-triggered splitting deformations of specific organic single crystals into small or fine crystal fragments are interesting from the perspective of crystal engineering [47–49]. However, these deformations occur randomly at crystal defects and are thus not suitable for top–down-controlled crystal shaping. Laser fabrication of microcrystals into nanoparticles is a common top–down approach [50], but this method is complex and can only

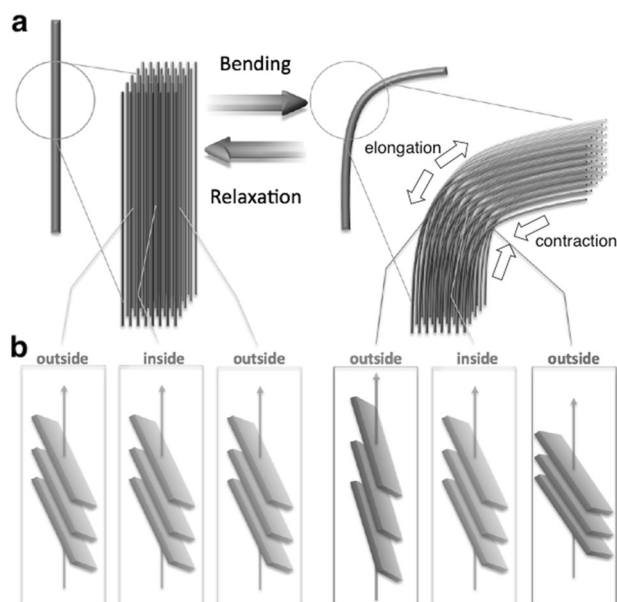


Fig. 2 Schematic illustration of a “fibril lamella” crystal. **a** Bending–relaxation motion. **b** Change in the center-to-center distance of π -CMs, resulting from the deformation of molecular wires

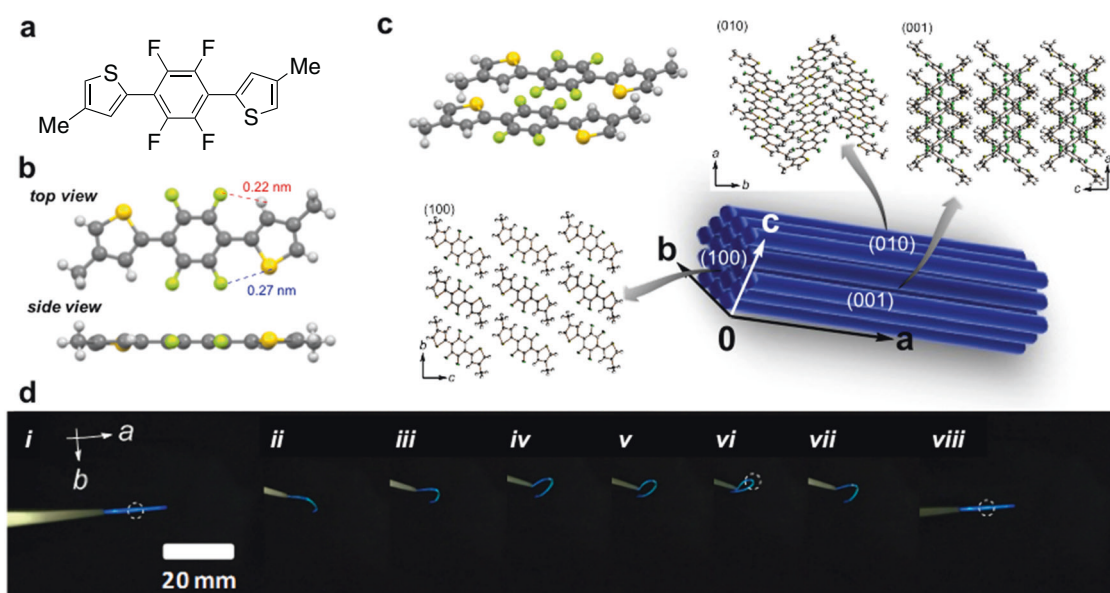


Fig. 3 **a** 1,4-Bis[2-(4-methylthienyl)]-2,3,5,6-tetrafluorobenzene, **1**. **b** Crystal structure. **c** Molecular packing and morphology in the crystal. **d** Elastic bending motion of the crystal. Figures adapted with permission from ref. [41], Wiley–VCH

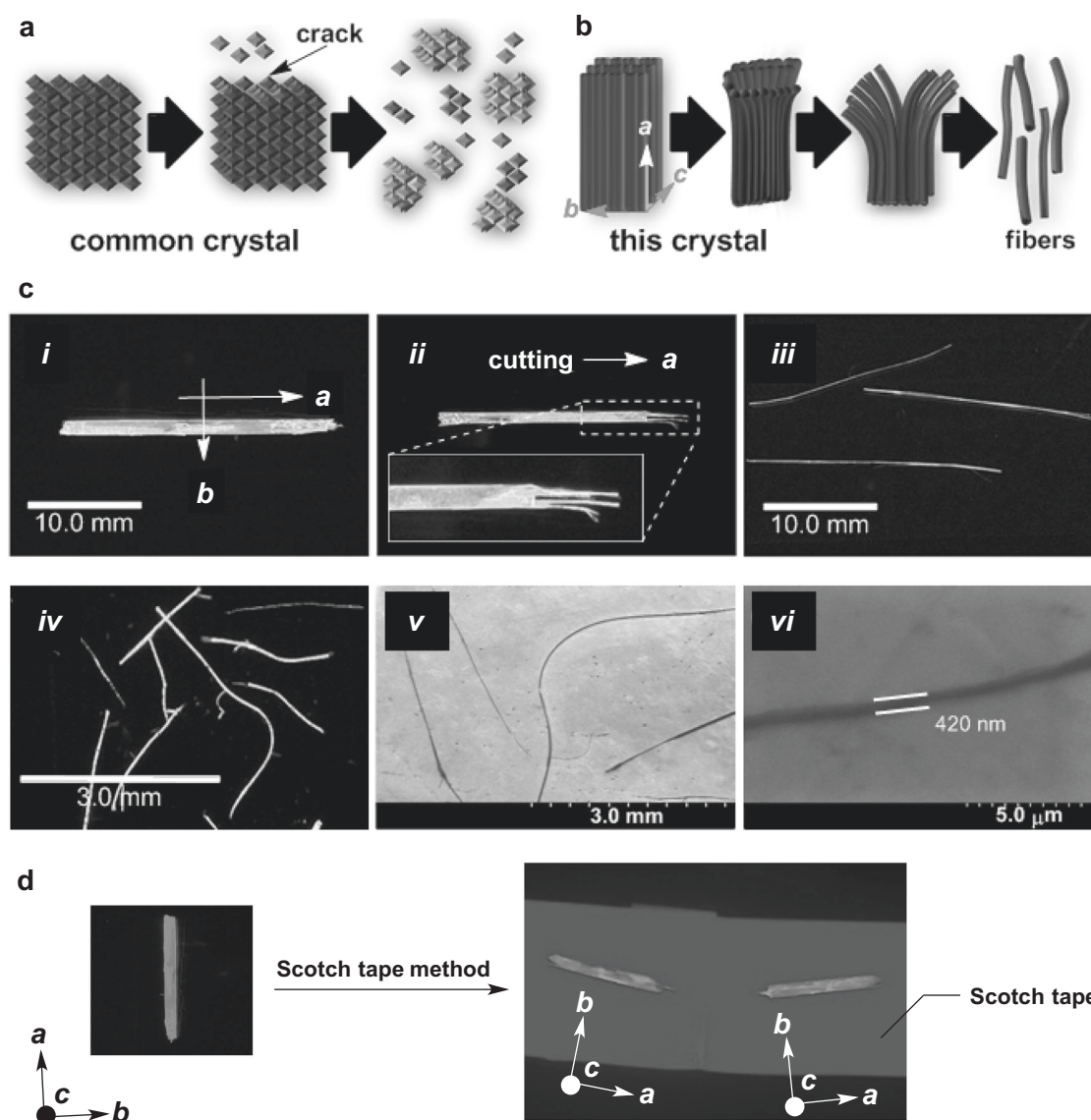


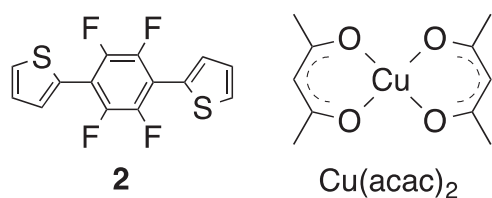
Fig. 4 **a** Illustration of the common organic crystal breakage under applied stress. **b** Illustration of the mechanical shaping of a single crystal of **1** into crystal fibers. **c** Photographic images of a crystal of **1** under UV (365 nm) irradiation: (i) a crystal of **1**; (ii) cutting the top of the crystal; (iii) the fabricated fine and long fibers; (iv) the fabricated

fine and short fibers. SEM images: (v) the fabricated fine and long fibers and (vi) a nanometer-scale fiber. **d** Fabrication of a crystalline film via the Scotch tape method. Figures adapted with permission from ref. [43], Wiley-VCH

produce nanoscale crystals. Mechanical shaping is an ideal process for preparing organic devices, but the brittleness of typical crystals makes it difficult to produce the exact shapes that are desired for use in specific devices. However, if large-scale (i.e., greater than micrometer scale) organic crystals could be endowed with elastic bending flexibility, organic single crystals could be easily processed into various fine shapes, such as fibers, via mechanical shaping.

Mechanically induced shaping (i.e., top-down processing) of organic single crystals is an undeveloped area of research, because applying stress to nonflexible crystalline materials generally causes them to disintegrate (Fig. 4a). The author has described a mechanical splitting phenomenon of the elastic

organic single crystal **1**, and a facile shaping method for centimeter-scale elastic organic single crystals of a fluorescent π -CM into various fine crystalline fibers (thickness: $\sim 50 \mu\text{m}$; width: $\sim 150 \mu\text{m}$; length: $\sim 25 \text{mm}$) (Fig. 4b, c). The fibers produced maintained their original crystal structure and properties (i.e., fluorescence efficiency and elastic flexibility). Thus, these long, fine, flexible, fluorescent organic single-crystal fibers show potential for applications in optoelectronics. Moreover, crystalline films could be prepared using the Scotch tape method (Fig. 4d) [43]. Elastic organic single crystals provide a new approach for crystal fibers and films, namely, the top-down synthesis of supramolecular 1D and 2D polymers [43].



Scheme 1 Chemical structures of 1,4-bis(2-thienyl)-2,3,5,6-tetrafluorobenzene **2** and $\text{Cu}(\text{acac})_2$

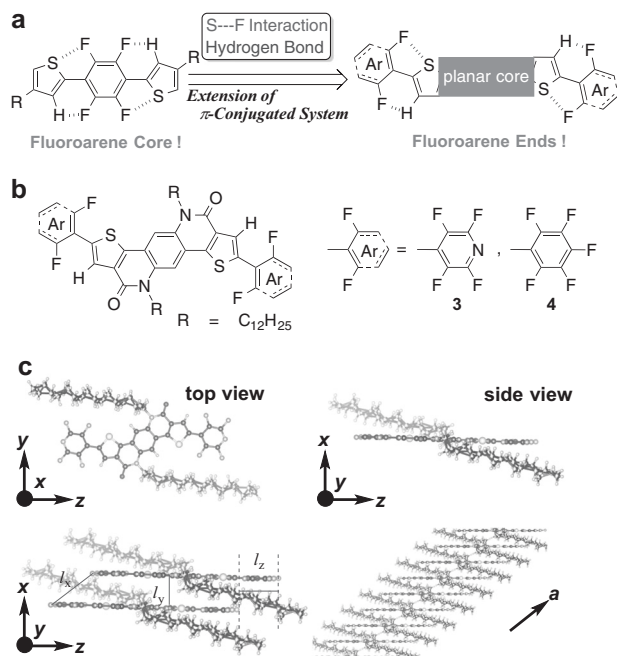


Fig. 5 **a** Design concepts. **b** Chemical structure. **c** Crystal structure of **3**. Figures adapted with permission from ref. [52], Wiley-VCH

Mechanically induced shaping can be performed on elastic organic single crystals with similar crystal morphologies to **1**, and can be carried out using other elastic crystals, such as 1,4-bis(2-thienyl)-2,3,5,6-tetrafluorobenzene **2** [42] and $\text{Cu}(\text{acac})_2$ (Scheme 1), which show fibril lamella crystal morphologies.

Elastic organic crystals of extended π -CMs with flexible optical waveguide

On the basis of this design strategy for elastic crystals (Fig. 2), the author previously found that two concerted intramolecular interactions ($\text{S}\cdots\text{F}$ contacts and hydrogen bonding) enhance the molecular planarity and rigidity (Fig. 2). To create elastic organic crystals, the author next focused on a related but further extended π -conjugated framework with a large planar core and fluoroarene termini

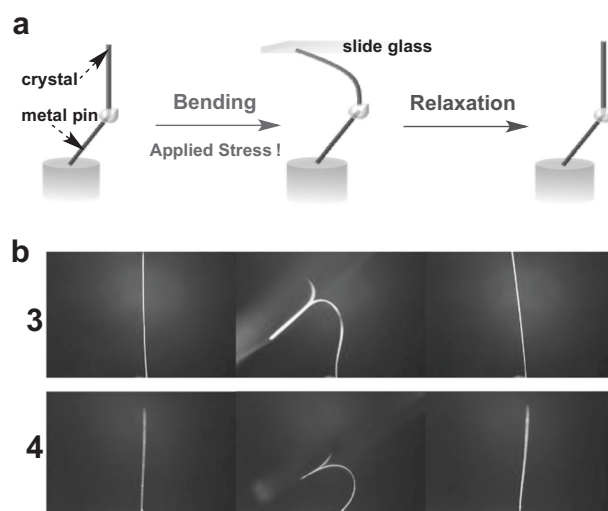


Fig. 6 **a** Illustration of the crystal fixed on a metal pin and the mechanical test. **b** Mechanical bending and relaxation of the crystals **3** and **4**. Stress was applied by pushing the crystal with a glass plate under UV (365 nm) irradiation. Figures adapted with permission from ref. [52], Wiley-VCH

(Fig. 5a, b) [51, 52]. The crystal structure of **3** is shown in Fig. 5c. The interatomic distance between S and F is 0.271 nm, which indicates intramolecular $\text{S}\cdots\text{F}$ interactions. The author also observed hydrogen bonding between H and F ($d = 0.220$ nm). The small torsion angle between the core and the fluoroarene units (2.16°) indicates an extended π -conjugated structure with high planarity and rigidity. The packing of the molecules showed a slip-stacked assembly along the *a* axis, supported by successive $\text{F}\cdots\text{F}$ halogen bonding interactions, which resulted in close π - π -stacking interactions ($l_y = 0.353$ nm) (Fig. 5c). The center-to-center distance of the molecular planes (l_z) is 0.434 nm. The fibril lamella morphology originates from the slip-stacked molecular wires through the self-assembly of planar molecules and crisscross packing [42] as viewed from the (010) face. The single-crystal structure of **4** also shows an intramolecular $\text{S}\cdots\text{F}$ interaction and hydrogen bonding. However, the torsion angle between the core unit and fluoroarene unit (11.36°) was greater than that of **3** (Fig. 5c).

Individual crystals were subjected to a mechanical test to assess their elastic features (Fig. 6a). The single crystals **3** and **4** were fixed on a metal pin with adhesive. Figure 6b shows the mechanical bending performance. Bending stress was applied by pushing the crystal with a glass plate. The straight-shaped crystal bent under applied stress in the *b* direction and recovered its original straight shape upon releasing the stress. Notably, this reversible bending-relaxation of the crystal could be cycled many times. This mechanical motion clearly indicates that the crystals are elastic (bending) organic single crystals. The crystal bending angle exceeded ca. 180° .

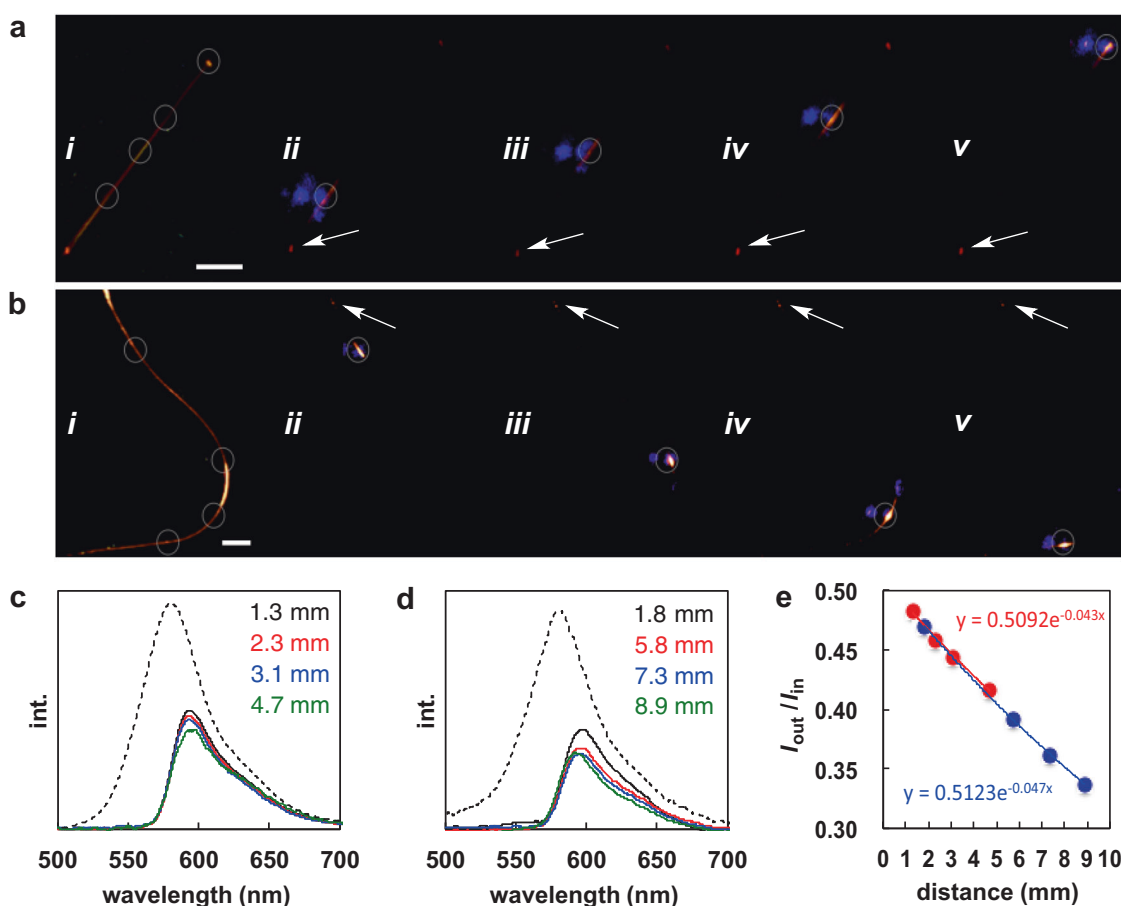


Fig. 7 Optical waveguide behavior of a crystal of **1** on a glass plate. **a** Straight crystal. **b** Bent crystal with 1.9% strain. Scale bar: 1 mm. **c** Emission spectra at the end of a straight crystal. Dotted line: emission spectrum at the illuminated position. **d** Emission spectra at the end of a

bent single crystal. Dotted line: emission spectrum at the illuminated position. **e** Relative $I_{\text{out}}/I_{\text{in}}$ values as a function of the distance from the illuminated position to the end. Red: straight crystal. Blue: Bent crystal. Figures adapted with permission from ref. [52], Wiley-VCH

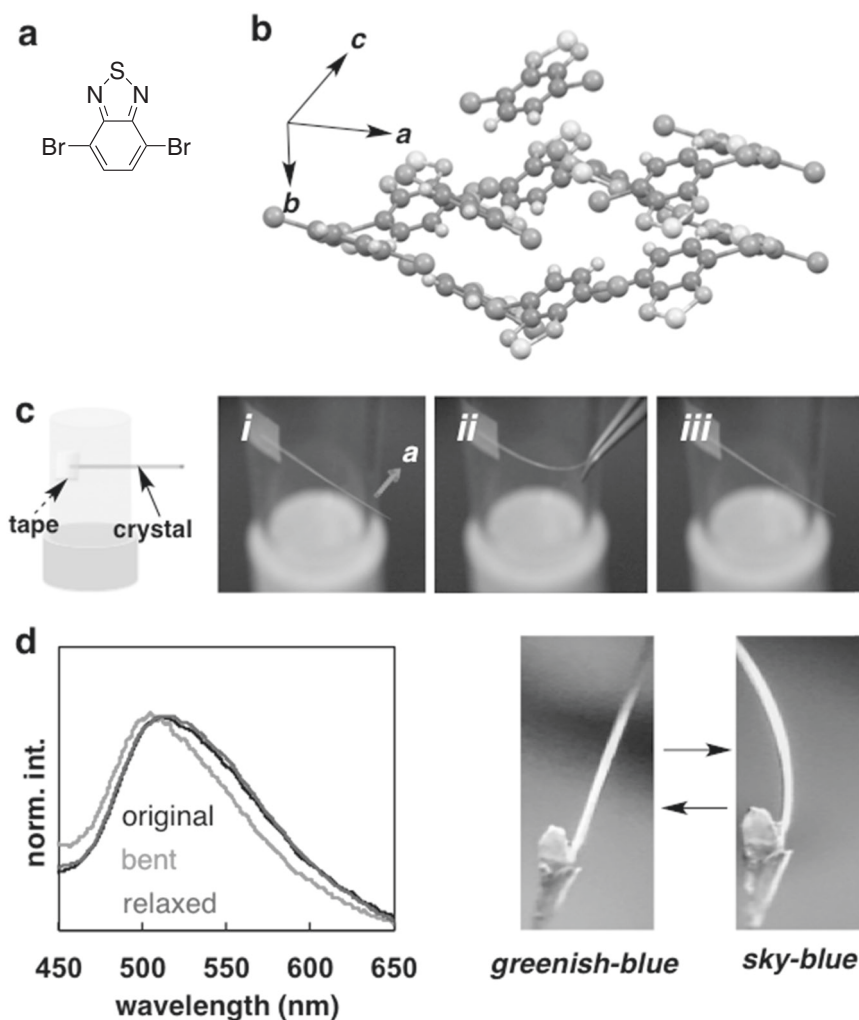
The author found that the single crystals exhibited unique optical waveguide (OWG) characteristics (Fig. 7) [52]. The refractive index and a low amount of surface defects are very important factors for high-performance OWG [53]. Organic crystals of π -CMs are suitable OWG materials compared with π -conjugated polymers, but their crystals are generally less flexible. Thus, elastic crystals of π -CMs are considered to be suitable for high-performance and flexible OWG materials. By illuminating the straight crystal with a focused laser (405 nm) at different positions, reddish–orange emission was always detected from the end of the straight crystal **3**, irrespective of the excitation position (Fig. 7a). This is a typical characteristic of OWG materials [53–56]. The bent crystal **3**, in which the elastic strain (ϵ value) of the bent crystal was calculated to be 1.9%, also showed a comparable waveguide performance (Fig. 7b). Figure 7c, d show the emission spectra of the straight and the bent crystals, respectively, at the illuminated position (black dotted line) and at the end of the crystal (solid line). The emission band at the end of the crystal showed a peak at 597 nm with a narrower full-

width at half-maximum (FWHM: 34 nm) than at the illuminated position (573 nm, FWHM: 56 nm). The spectral profiles did not change substantially depending on the illumination position, although the emission intensity at the end very slightly decreased with increasing distance (Fig. 7c, d). The author measured the fluorescence intensities at the illuminated position (I_{in}) and at the end of the crystal (I_{out}) to calculate the optical loss coefficient by measuring the spatially resolved PL spectra and fitting by using a single exponential curve ($I_{\text{in}}/I_{\text{out}} = Ae^{(-\alpha X)}$, where X is the distance between the illuminated position and the end of the crystal, and α is the loss coefficient) [53–56]. The α values were thus calculated to be 0.043 and 0.047 dB/mm for the straight and bent crystals, respectively (Fig. 7e).

Reversible mechanical sensors

Another interesting feature of organic single crystals is the occurrence of mechanochromism and

Fig. 8 **a** Chemical structure of **DBBT**. **b** Crystal structure. **c** Bending–relaxation motion. **d** Bending mechanofluorochromism. Emission spectra and a photograph of the straight and the bent crystals. Figures adapted with permission from ref. [63], the American Chemical Society



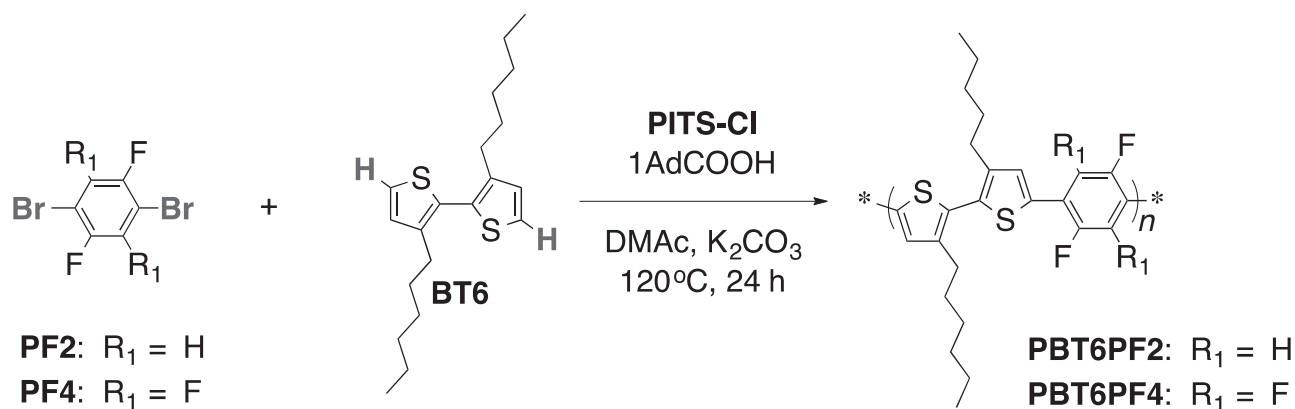
mechanofluorochromism [57–60]. The molecular orientation and intermolecular interactions in light-emitting crystals are perturbed by mechanical forces (e.g., shearing, grinding, tension, and hydrostatic pressure), which can cause a change in the emission color of the crystals. There have been few reports of reversible color changes under the application and release of mechanical stress (pressure) [61, 62], although this could be an important characteristic of these materials. Consequently, flexible and tough crystals of π -CMs are candidate materials for reversible mechanosensors.

The author has also studied a crystal of the commercially available 4,7-dibromo-2,1,3-benzothiadiazole, **DBBT** (Fig. 8a, b) [63]. A centimeter-scale needle-shaped single crystal of the molecule bends under applied stress and quickly reverts to its original shape upon relaxation; therefore, the material is an elastic organic single crystal (Fig. 8c). Moreover, the crystal shows greenish-blue colored fluorescence ($\lambda = 513$ nm, $\Phi =$ ca. 9%). In contrast, the crystal showed a slightly different spectrum ($\lambda = 504$ nm) and color (sky-blue) when it was mechanically bent near its elastic bending limit (30°) (Fig. 8d).

The unique mechanical and fluorescent properties of the crystal include mechanofluorochromism based on mechanical bending–relaxation cycles. The change in fluorescence is probably due to changing the center-to-center separation length in the slip-stacked molecular packing. The packing of **DBBT** shifts from stable to metastable during mechanical bending, resulting in a blue-shifted fluorescence band. Relaxation of the bent crystal allows the recovery of the stable packing mode.

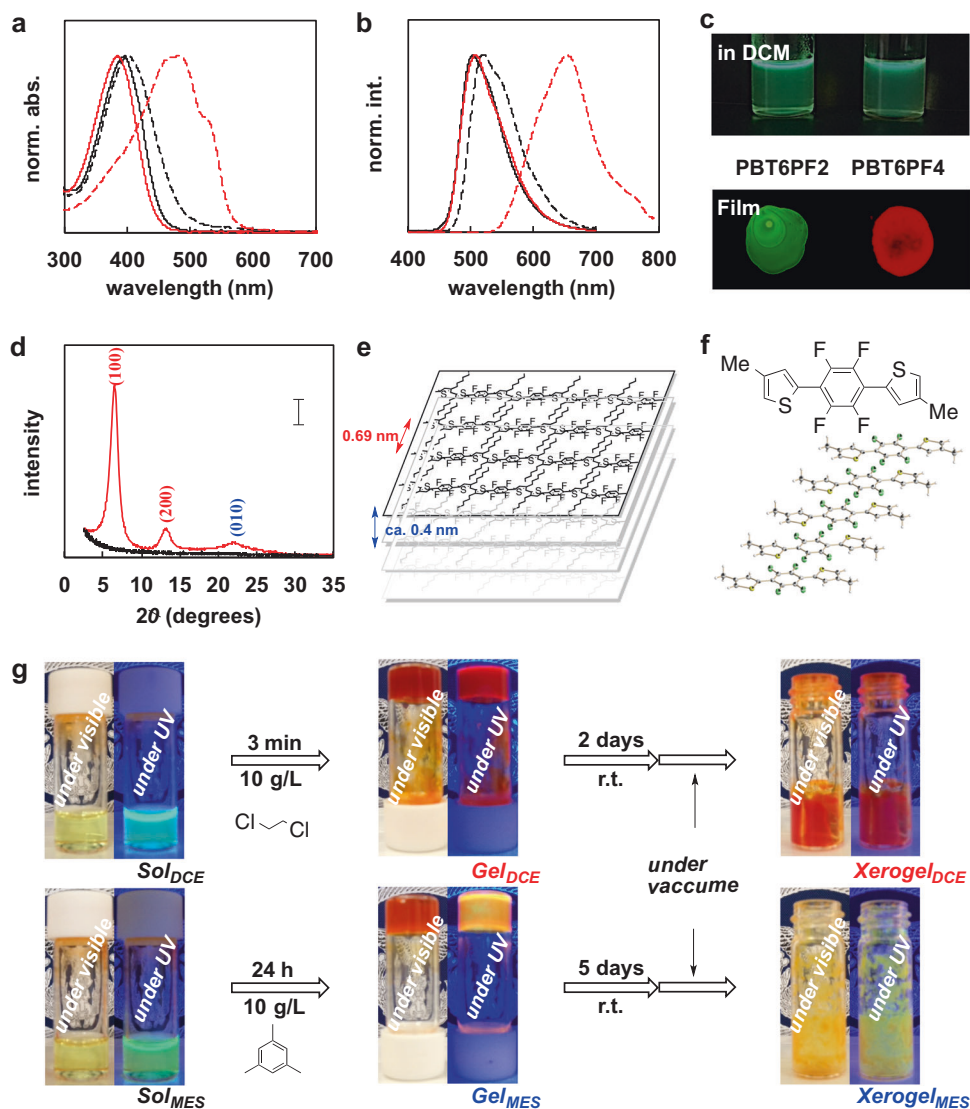
Solvent control of the supramolecular formation of π -conjugated polymers

Supramolecular (crystalline) structures based on π -conjugated polymers are of interest in the broad field of device applications [64–67]. The development of highly crystalline π -conjugated polymers [64–68] is important for controlling their optoelectronic properties. 1,4-Bis[2-(4-methylthienyl)]-2,3,5,6-tetrafluorobenzene, **1**, is simple and attractive for solid-state fluorescence and is a suitable monomer structure [41–43]. Thus, the author studied a π -conjugated



Scheme 2 Synthesis of **PBT6PF2** and **PBT6PF4** via DAoP

Fig. 9 **a** UV-Vis absorption spectra of **PBT6PF2** and **PBT6PF4** in DCM (solid line) and as a thin film (dotted line). **b** Fluorescence spectra of **PBT6PF2** and **PBT6PF4** in DCM (solid line) and as a thin film (dotted line). **c** Fluorescence images of **PBT6PF2** and **PBT6PF4**. **d** XRD patterns of **PBT6PF2** (black line) and **PBT6PF4** (red line). **e** A schematic illustration of the macrostructural order. Scale bar: 5000 counts. **f** The crystal structure of **1** showing the slip-stacked arrangement (*J*-aggregation). **g** Supramolecular gel formation of **PBT6PF4**. Sample tube: diameter = 1 cm, height = ca. 3 cm. Figures adapted with permission from ref. [76], Wiley-VCH



polymer formed from thiophene–tetrafluorobenzene repeating units. The author has also recently reported various π -conjugated polymer syntheses via direct arylation

polycondensation (DAoP) [69–75]. Thus, DAoP of 1,4-dibromo-2,3,5,6-tetrafluorobenzene **PF4** with 3,3'-dihexyl-2,2'-bithiophene **BT** gave a simple alternating copolymer,

PBT6PF4 (Scheme 2) [76]. Surprisingly, this polymer yielded a highly crystalline and fluorescent film (Fig. 9a–e). The alternating polymer **PBT6PF2** synthesized by DArP of 1,4-dibromo-3,5-difluorobenzene **PF2** with **BT** [75], however, does not show an ordered structure in the film state. In the film, the polymer exhibited efficient red-colored fluorescence, an improved quantum yield ($\Phi_{\text{sol}} = 13\% \rightarrow \Phi_{\text{film}} = 23\%$) and a crystalline structure. Its efficient fluorescence behavior is due to the J-aggregated packing structure of the thiophene–tetrafluorophenylene–thiophene units (Fig. 9f) [41–43]. Interestingly, supramolecular gel formation occurred in appropriate solvents, and the crystalline domain and fluorescence properties of the gel could be directly controlled by the choice of the solvent (Fig. 9g). The polymer self-assembled into a spherical form that exhibited red fluorescence in a non-aromatic solvent (1,2-dichloroethane) and into a fibrous form that exhibited yellow fluorescence in an aromatic solvent (mesitylene).

Final remarks

Organic crystalline supramolecular 3D polymers, bulk organic crystals, have attracted much attention owing to their potential applications in unique and/or high-performance organic devices. However, organic crystals are generally not flexible. Herein, the author's research on elastic organic crystals is introduced and discussed. The author developed an elastic organic crystal with π -functionality, which shows reversible bending flexibility and optical properties. The first disclosure of 1,4-bis[2-(4-methylthienyl)]-2,3,5,6-tetrafluorobenzene provided exciting new opportunities in flexible materials science, unique material applications, and top–down shape-tuning based on flexibility and π -conjugated molecular structures. In addition to the top–down shape-tuning of the elastic crystals, control over the supramolecular formation (bottom–up synthesis) of a π -conjugated polymer was described. This type of polymer could be designed by harnessing the properties of 1,4-bis[2-(4-methylthienyl)]-2,3,5,6-tetrafluorobenzene. This research will enable the development of new polymers and crystals with potential applications in various organic devices.

Acknowledgements I acknowledge a KAKENHI (Grant-in-Aid for Scientific Research B: no. 18H02052, and Grant-in Aid for Scientific Research on Innovative Areas “ π -figuration”: no. 17H05171) from the Japan Society for the Promotion of Science (JSPS). This work was performed under the Cooperative Research Program of the “Network Joint Research Center for Materials and Devices”. I thank Alison McGonagle, PhD, from Edanz (www.edanzediting.com/ac) for editing a draft of this manuscript.

Compliance with ethical standards

Conflict of interest The authors declare that they have no conflict of interest.

Publisher's note: Springer Nature remains neutral with regard to jurisdictional claims in published maps and institutional affiliations.

References

1. Wang C, Dong H, Hu W, Liu Y, Zhu D. Semiconducting π -conjugated systems in field-effect transistors: a material odyssey of organic electronics. *Chem Rev.* 2012;112:2208–67.
2. Gidron O, Bendikov M. α -Oligofurans: an emerging class of conjugated oligomers for organic electronics. *Angew Chem Int Ed.* 2014;53:2546–55.
3. Kobaisi MA, Bhosale SV, Latham K, Raynor AM, Bhosale SV. Functional naphthalene diimides: synthesis, properties, and applications. *Chem Rev.* 2016;116:11685–11796.
4. Gao F, Liao Q, Xu Z-Z, Yue Y-H, Wang Q, Zhang H-L, et al. Strong two-photon excited fluorescence and stimulated emission from an organic single crystal of an oligo (phenylene vinylene). *Angew Chem Int Ed.* 2010;49:732–5.
5. Omachi H, Segawa Y, Itami K. Synthesis of cyclophenylenes and related carbon nanorings: a step toward the controlled synthesis of carbon nanotubes. *Acc Chem Res.* 2012;45:1378–89.
6. Holzwarth J, Amsharov KY, Sharapa DI, Reger D, Roschyna K, Lungerich D, et al. Highly regioselective alkylation of hexabenzocoronenes: fundamental insights into the covalent chemistry of graphene. *Angew Chem Int Ed.* 2017;56:12184–90.
7. Hayashi S, Sakamoto M, Ishiwari F, Fukushima T, Yamamoto S, Koizumi T. A versatile scaffold for facile synthesis of fluorescent cyano-substituted stilbenes. *Tetrahedron.* 2019;75:1079–84.
8. Hayashi S, Koizumi T. From benzodiazaborole-based compound to donor-acceptor polymer via electropolymerization. *Polym Chem.* 2012;3:613–6.
9. Hayashi S, Hirai R, Yamamoto S, Koizumi T. A simple route to unsymmetric cyano-substituted oligo(p-phenylene-vinylene)s. *Chem Lett.* 2018;47:1003–5.
10. Hayashi S, Yamamoto S, Koizumi T. A cyclic compound based on xanthene-linked π -dimer via direct arylation. *Chem Lett.* 2017;46:200–3.
11. Santhosh Babu S, Praveen VK, Ajayaghosh A. Functional π -gelators and their applications. *Chem Rev.* 2014;114:1973–2129.
12. Ajayaghosh A, Praveen VK. π -Organogels of self-assembled p-phenylenevinylene: soft materials with distinct size, shape, and functions. *Acc Chem Res.* 2007;40:644–56.
13. Ishiwari F, Shoji Y, Fukushima T. Supramolecular scaffolds enabling the controlled assembly of functional molecular units. *Chem Sci.* 2018;9:2028–41.
14. Kang J, Miyajima D, Mori T, Inoue Y, Itoh Y, Aida T. Noncovalent assembly. A rational strategy for the realization of chain-growth supramolecular polymerization. *Science.* 2015;347:646–51.
15. Ogi S, Sugiyasu K, Manna S, Samitsu S, Takeuchi M. Living supramolecular polymerization realized through a biomimetic approach. *Nat Chem.* 2014;6:188–95.
16. Seiki N, Shoji Y, Kajitani T, Ishiwari F, Kosaka A, Hikima T, et al. Rational synthesis of organic thin films with exceptional long-range structural integrity. *Science.* 2015;348:1122–6.
17. Leung FK-C, Ishiwari F, Kajitani T, Shoji Y, Hikima T, Takata M, et al. Supramolecular scaffold for tailoring the two-dimensional assembly of functional molecular units into organic thin films. *J Am Chem Soc.* 2016;138:11727–33.
18. Inada Y, Yamao T, Inada M, Itami T, Hotta S. Giant organic single-crystals of a thiophene/phenylene co-oligomer toward device applications. *Synth Met.* 2011;161:1869–77.
19. Reese C, Bao Z. Organic single crystals: tools for the exploration of charge transport phenomena in organic materials. *J Mater Chem.* 2006;16:329–33.

20. Dove, MT Structure and dynamics: an atomic view of materials (Oxford University Press, 2003).
21. Kahr B, Ward MD. Stressed out crystals. *Nat Chem.* 2018;10:4–6.
22. Worthy A, Grosjean A, Pfrunder MC, Xu Y, Yan C, Edwards G, et al. Atomic resolution of structural changes in elastic crystals of copper(II) acetylacetonate. *Nat Chem.* 2018;10:65–69.
23. De Boer RWI, Gershenson ME, Morpurgo AF, Podzorov V. Organic single-crystal field-effect transistors. *Phys Stat Sol A.* 2004;201:1302–31.
24. Sundar VC, Zaumseil J, Podzorov V, Menard E, Willett RL, Someya T, et al. Elastomeric transistor stamps: reversible probing of charge transport in organic crystals. *Science.* 2004;303:1644–6.
25. Wang H, Deng L, Tang Q, Tong Y, Liu Y. Flexible organic single-crystal field-effect transistor for ultra-sensitivity strain sensing. *IEEE Electron Device Lett.* 2017;38:1598–601.
26. Cheng Y-J, Yang S-H, Hsu C-S. Synthesis of conjugated polymers for organic solar cell applications. *Chem Rev.* 2009;109:5868–923.
27. Thomas SW III, Joly GD, Swager TM. Chemical sensors based on amplifying fluorescent conjugated polymers. *Chem Rev.* 2007;107:1339–86.
28. Beaujuge PM, Reynolds JR. Color control in π -conjugated organic polymers for use in electrochromic devices. *Chem Rev.* 2010;110:268–320.
29. Hayashi S, Nishioka N, Nishiyama H, Koizumi T. π -Conjugated alternating copolymer based on the 3,5-dinitro-9-fluorenone for electron-acceptor type materials. *Synth Met.* 2012;162:1485–9.
30. Hayashi S, Koizumi T. Modification of pyridine-based conjugated polymer films via Lewis acid: halochromism, characterization and macroscopic gradation patterning. *Polym Chem.* 2011;2:2764–6.
31. Hayashi S, Koizumi T. Two synthetic approaches from di(thien-2-yl)-2,5-pyridine to a BF_3 -modified polymer film. *Chem Lett.* 2012;41:979–81.
32. Hayashi S, Inagi S, Fuchigami T. Synthesis of 9-substituted fluorene copolymers via chemical and electrochemical polymer reaction and their optoelectronic properties. *Macromolecules.* 2009;42:3755–60.
33. Hayashi S, Yamamoto S, Koizumi T. Effects of molecular weight on the optical and electrochemical properties of EDOT-based π -conjugated polymers. *Sci Rep.* 2017;7:1027.
34. Ahmed E, Karothu DP, Naumov P. Crystal adaptronics: mechanically reconfigurable elastic and superelastic molecular crystals. *Angew Chem Int Ed.* 2018;57:8837–46.
35. Lv S, Dudek DM, Cao Y, Balamureli MM, Gosline J, Li H. Designed biomaterials to mimic the mechanical properties of muscles. *Nature.* 2010;465:69–73.
36. Reddy CM, Krishna GR, Ghosh S. Mechanical properties of molecular crystals—applications to crystal engineering. *CrytEngComm.* 2010;12:2296–314.
37. Ghosh S, Reddy CM. Elastic and bendable caffeine cocrystals: implications for the design of flexible organic materials. *Angew Chem Int Ed.* 2012;51:10319–23.
38. Facchetti A, Yoon M-H, Stern CL, Katz HE, Marks TJ. Building blocks for n-type organic electronics: regiochemically modulated inversion of majority carrier sign in perfluoroarene-modified polythiophene semiconductors. *Angew Chem Int Ed.* 2003;42:3900–3.
39. Crouch DJ, Skabara PJ, Heeney M, McCulloch I, Coles, SJ & Hursthouse, MB. Hexyl-substituted oligothiophenes with a central tetrafluorophenylene unit: crystal engineering of planar structures for p-type organic semiconductors. *Chem. Commun.* 1465–7 (2005).
40. Crouch DJ, Skabara PJ, Lohr JE, McDouall JJW, Heeney M, McCulloch I, et al. Thiophene and selenophene copolymers incorporating fluorinated phenylene units in the main chain: synthesis, characterization, and application in organic field-effect transistors. *Chem Mater.* 2005;17:6567–78.
41. Hayashi S, Koizumi T. Elastic organic crystal of a fluorescent π -conjugated molecule. *Angew Chem Int Ed.* 2016;55:2701–4.
42. Hayashi S, Asano A, Kamiya N, Yokomori Y, Maeda T, Koizumi T. Fluorescent organic single crystals with elastic bending flexibility: 1,4-bis(thien-2-yl)-2,3,5,6-tetrafluorobenzene derivatives. *Sci Rep.* 2017;7:9453.
43. Hayashi S, Koizumi T. Mechanically induced shaping of organic single crystals: facile fabrication of fluorescent and elastic crystal fibers. *Chem Eur J.* 2018;24:8507–12.
44. Hoeben FJM, Jonkheijm P, Meijer EW, Schenning APHJ. About supramolecular assemblies of π -conjugated systems. *Chem Rev.* 2005;105:1491–1546.
45. Chen W, Qi D-C, Huang H, Gao X, Wee ATS. Organic–organic heterojunction interfaces: effect of molecular orientation. *Adv Funct Mater.* 2011;21:410–24.
46. Yu Z, Wu Y, Liao Q, Zhang H, Bai S, Li H, et al. Self-assembled microdisk lasers of perylenediimides. *J Am Chem Soc.* 2015;137:15105–11.
47. Naumov P, Sahoo SC, Zakharov BA, Boldyreva EV. Dynamic single crystals: kinematic analysis of photoinduced crystal jumping (the photosalient effect). *Angew Chem Int Ed.* 2013;53:9990–5.
48. Ghosh S, Mishre MK, Ganguly S, Desiraju GR. *J Am Chem Soc.* 2015;137:9912–21.
49. Zhang Y, Peng C, Zhou Z, Duan R, Che HJY, Zhao J. Giant morphological change in layered microribbons featuring reversible sliding of stacking layers. *Adv Mater.* 2015;27:320–5.
50. Asahi T, Sugiyama T, Msuhara H. Laser fabrication and spectroscopy of organic nanoparticles. *Acc Chem Res.* 2008;41:1790–8.
51. Takagi K, Yamamoto S, Tsukamoto K, Hirano Y, Hara M, Nagano S, et al. Synthesis and field-effect transistor application of π -extended lactam-fused conjugated oligomers obtained by tandem direct arylation. *Chem Eur J.* 2018;24:14137–45.
52. Hayashi S, Yamamoto S, Takeuchi D, Ie Y, Takagi K. Creating elastic organic crystals of π -conjugated molecules with flexible optical waveguide and bending mechanofluorochromism. *Angew Chem Int Ed.* 2019;57:17002–8.
53. Zhang C, Sheng Y, Yao J. Optical waveguides at micro/nanoscale based on functional small organic molecules. *Phys Chem Chem Phys.* 2011;13:9060–73.
54. Hayashi S, Koizumi T, Kamiya N. 2,5-Dimethoxybenzene-1,4-dicarboxaldehyde: an emissive organic crystal and highly efficient fluorescent waveguide. *ChemPlusChem.* 2019;84:247–51.
55. Li Y, Ma Z, Li A, Xu W, Wang Y, Jiang H, et al. A single crystal with multiple functions of optical waveguide, aggregation-induced emission, and mechanochromism. *ACS Appl Mater Interfaces.* 2017;9:8910–8918.
56. Guo Z-H, Lei T, Jin Z-X, Wang J-Y, Pei J. T-Shaped donor–acceptor molecules for low-loss red-emission optical waveguide. *Org Lett.* 2013;15:3530–3.
57. Sagara Y, Kato T. Mechanically induced luminescence changes in molecular assemblies. *Nat Chem.* 2009;1:605–10.
58. Chi Z, Zhang X, Xu B, Zhou X, Ma C, Zhang Y, et al. Recent advances in organic mechanofluorochromic materials. *Chem Soc Rev.* 2012;41:3878–96.
59. Ito S, Yamada T, Taguchi T, Yamaguchi Y, Asami M. *N*-Boc-indolylbenzothiadiazole derivatives: efficient full-color solid-state fluorescence and self-recovering mechanochromic luminescence. *Chem Asian J.* 2016;11:1963–70.
60. Sharber SA, Shih K-C, Mann A, Frausto F, Haas TE, Nieh M-P, et al. Reversible mechanofluorochromism of aniline-terminated phenylene ethynyls. *Chem Sci.* 2008;9:5415–26.
61. Nagura K, Saito S, Yusa H, Yamawaki H, Fujihisa H, Sato H, et al. Distinct responses to mechanical grinding and hydrostatic

- pressure in luminescent chromism of tetrathiazolylthiophene. *J Am Chem Soc.* 2013;135:10322–5.
62. Ono T, Tsukiyama Y, Taema A, Sato H, Kiyooka H, Yamaguchi Y, et al. Piezofluorochromism in charge-transfer inclusion crystals: the influence of high pressure versus mechanical grinding. *ChemPhotoChem.* 2018;2:416–20.
63. Hayashi S, Koizumi T, Kamiya N. Elastic bending flexibility of fluorescent organic single crystal: new aspects of commonly used building block “4,7-dibromo-2,1,3-benzothiadiazole”. *Cryst Growth Des.* 2017;17:6158–62.
64. Xia, D, Li, C & Li, W. Crystalline conjugated polymers for organic solar cells: from donor, acceptor to single-component. *Chem. Record:* <https://doi.org/10.1002/tcr.201800131>.
65. Osaka I, Takimiya K. Crystalline conjugated polymers for organic electronics. *IOP Conf Ser Mater Sci Eng.* 2014;54:012016.
66. Chung K, Yu Y, Kwon MS, Swets J. Assembly and alignment of conjugated polymers: materials design, processing, and applications. *MRS Commun.* 2015;5:169–89.
67. Rahimi K, Botiz I, Stingelin N, Kayunkid N, Sommer M, Koch FPV, et al. Controllable processes for generating large single crystals of poly(3-hexylthiophene). *Angew Chem Int Ed.* 2012;51:11131–5.
68. Hayashi S, Inagi S, Fuchigami T. Macrostructural order and optical properties of polyfluorene-based polymer films. *Polym J.* 2010;42:772–5.
69. Hayashi S, Kojima Y, Koizumi T. Highly regioselective Pd/C-catalyzed direct arylation toward thiophene-based π -conjugated polymers. *Polym Chem.* 2015;6:5036–9.
70. Yasuda T, Imase T, Sakai S, Yamamoto T. Synthesis, solid structure, and optical properties of new thiophene-based alternating p-conjugated copolymers containing 4-alkyl-1,2,4-triazole or 1,3,4-thiadiazole unit as the partner unit. *Macromolecules.* 2005;38:1500–3.
71. Hayashi S. Direct arylation for the control of π -conjugated polymer structure. *Kobunshi Ronbunshu.* 2017;74:375–95.
72. Hayashi S, Kojima Y, Koizumi T. Direct arylation polycondensation of β -unprotected chalcogen heteroles under phosphine-free conditions. *Polym (Guildf).* 2017;113:214–20.
73. Hayashi S, Togawa Y, Kojima Y, Koizumi T. Direct arylation of fluoroarenes toward linear, bent-shaped and branched π -conjugated polymers: polycondensation and post-polymerization approaches. *Polym Chem.* 2016;7:5671–86.
74. Hayashi S, Koizumi T. Chloride-promoted Pd-catalyzed direct C–H arylation for highly efficient phosphine-free synthesis of π -conjugated polymers. *Polym Chem.* 2015;6:5036–9.
75. Hayashi S, Takigami A, Koizumi T. Palladium-immobilized on thiol-modified silica gel: an effective catalyst for direct arylation approach. *ChemPlusChem.* 2016;7:5671–86.
76. Hayashi S, Takigami A, Koizumi T. Solvent control over supramolecular gel formation and fluorescence for a highly crystalline π -conjugated polymer. *Chem Asian J.* 2018;13:2014–8.



Shotaro Hayashi is currently an associate professor in the Department of Applied Chemistry at the National Defense Academy. He was born in Hiroshima, Japan in 1982. He received a Ph.D (2010) from the Tokyo Institute of Technology. He moved to the National Defense Academy as an assistant professor in 2010. He has received the Nippon Shokubai Co., Ltd. Award in Synthetic Organic Chemistry, Japan (2015) and the Award for the Encouragement of Research in Polymer Science from the Society of Polymer Science, Japan (2018). His current research interests are (i) supramolecular polymers and crystals of π -conjugated molecules, and (ii) Pd-catalyzed cross-coupling synthesis of π -conjugated polymers.